Rosiglitazone accelerates wound healing by improving endothelial precursor cell function in *db/db* mice

Guoliang Zhou [Equal first author, 1], Xue Han [Equal first author, 2], Zhiheng Wu [3], Qiaojuan Shi [Corresp., 2], Xiaogang Bao [Corresp. 4]

[1] Department of Pharmacy, School of Life and Health Sciences, Anhui Science and Technology University, Fengyang, Anhui, China

[2] Laboratory Animal Center, Zhejiang Academy of Medical Sciences, Hangzhou, Zhejiang Province, China

[3] School of clinical medicine, Wannan Medicial Colledge, Wuhu, Anhui, China

[4] Department of Orthopedic Surgery, Spine Center, Changzheng Hospital, Second Military Medical University, Shanghai, China

Corresponding Authors: Qiaojuan Shi, Xiaogang Bao
Email address: shiqiaojuan@163.com, bxg1832178@smmu.edu.cn

Background & Aims. Endothelial precursor cell (EPC) dysfunction is one of the risk factors for diabetes mellitus (DM) which results in delayed wound healing. Rosiglitazone (RSG) is a frequently prescribed oral glucose-lowering drug. Previous studies have shown the positive effects of RSG on ameliorating EPC dysfunction in diabetic patients. Interestingly, knowledge about RSG with regard to the wound healing process caused by DM is scarce. Therefore, in this study, we investigated the possible actions of RSG on wound healing and the related mechanisms involved in *db/db* diabetic mice. **Methods.** *Db/db* mice with spontaneous glucose metabolic disorder were used as a type 2 DM model. RSG (20mg/kg/d, *i.g.*) was administered for 4 weeks before wound creation and bone marrow derived EPC (BM-EPC) isolation. Wound closure was assessed by wound area and CD31 staining. Tubule formation and migration assays were used to judge the function of the BM-EPCs. The level of vascular endothelial growth factor (VEGF), stromal cell derived factor-1α (SDF-1α) and insulin signaling was determined by ELISA. Cell viability of the BM-EPCs was measured by CCK-8 assay. **Results.** RSG significantly accelerated wound healing and improved angiogenesis in *db/db* mice. Bioactivities of tube formation and migration were decreased in *db/db* mice but were elevated by RSG. Level of both VEGF and SDF-1α was increased by RSG in the BM-EPCs of *db/db* mice. Insulin signaling was elevated by RSG reflected in the phosphorylated-to-total AKT in the BM-EPCs. *In vitro*, RSG improved impaired cell viability and tube formation of BM-EPCs induced by high glucose, but this was prevented by the VEGF inhibitor avastin. **Conclusion.** Our data demonstrates that RSG has benefits for wound healing and angiogenesis in diabetic mice, and was partially associated with improvement of EPC function through activation of VEGF and stimulation of SDF-1α in *db/db* mice.

1 Rosiglitazone accelerates wound healing by improving

2 endothelial precursor cell function in *db/db* mice

3 Guoliang Zhou[1,*], Xue Han[2,*], Zhiheng Wu[3], Qiaojuan[2,#] Shi, Xiaogang Bao[4,#]

4 [1] Department of Pharmacy, School of Life and Health Sciences, Anhui Science and Technology

5 University, Fengyang, Anhui Province, China

6 [2] Laboratory Animal Center, Zhejiang Academy of Medical Sciences, Hangzhou, Zhejiang

7 Province, China

8 [3] School of clinical medicine, Wannan Medicial Colledge, Wuhu, Anhui Province, China

9 [4] Department of Orthopedic Surgery, Spine Center, Changzheng Hospital, Second Military

10 Medical University, Shanghai, China

11 *These authors contributed equally to this work.

13 Corresponding Author:

14 Xiaogang Bao[4,#]

15 415 Fengyang Road, Shanghai, 200003, China

16 Email address: bxg1832178@smmu.edu.cn

17 Co-corresponding Author:

18 Qiaojuan Shi[2,#]

19 182 Tianmushan Road, Hangzhou, Zhejiang Province, 310013, China

20 Email address: shiqiaojuan@163.com

22
23
24
25
26
27
28
29
30
31
32
33
34
35
Abstract

Background & Aims. Endothelial precursor cell (EPC) dysfunction is one of the risk factors for diabetes mellitus (DM) which results in delayed wound healing. Rosiglitazone (RSG) is a frequently prescribed oral glucose-lowering drug. Previous studies have shown the positive effects of RSG on ameliorating EPC dysfunction in diabetic patients. Interestingly, knowledge about RSG with regard to the wound healing process caused by DM is scarce. Therefore, in this study, we investigated the possible actions of RSG on wound healing and the related mechanisms involved in *db/db* diabetic mice.

Methods. *Db/db* mice with spontaneous glucose metabolic disorder were used as a type 2 DM model. RSG (20mg/kg/d, *i.g.*) was administered for 4 weeks before wound creation and bone marrow derived EPC (BM-EPC) isolation. Wound closure was assessed by wound area and CD31 staining. Tubule formation and migration assays were used to judge the function of the BM-EPCs. The level of vascular endothelial growth factor (VEGF), stromal cell derived factor-1α (SDF-1α) and insulin signaling was determined by ELISA. Cell viability of the BM-EPCs was measured by CCK-8 assay.

Results. RSG significantly accelerated wound healing and improved angiogenesis in *db/db* mice. Bioactivities of tube formation and migration were decreased in *db/db* mice but were elevated by RSG. Level of both VEGF and SDF-1α was increased by RSG in the BM-EPCs of *db/db* mice. Insulin signaling was elevated by RSG reflected in the phosphorylated-to-total AKT in the BM-EPCs. *In vitro*, RSG improved impaired cell viability and tube formation of BM-EPCs induced by high glucose, but this was prevented by the VEGF inhibitor avastin.

Conclusion. Our data demonstrates that RSG has benefits for wound healing and angiogenesis in diabetic mice, and was partially associated with improvement of EPC function through activation of VEGF and stimulation of SDF-1α in *db/db* mice.

Subjects Diabetes and Endocrinology, Pharmacology

Keywords Diabetes mellitus, Rosiglitazone, Endothelial precursor cell, Angiogenesis, Wound healing, Vascular endothelial growth factor

Introduction

Diabetes mellitus (DM) can cause serious complications, including cardiovascular and cerebrovascular disease, kidney disorders, and diabetic foot ulcers (DFU; Wan et al., 2019). With the worldwide prevalence of DM and increasing life-spans of diabetic patients, the number of individuals suffering from DFUs has dramatically increased (Evran Olgun et al., 2019). Previous studies have shown that the morbidity of foot ulceration in a DM cohort is approximately 15% to 20% in a person's lifetime (Abbott et al,. 2002), and the average annual cost of this refractory disease is $8,659 per patient (Tennvall & Apelqvist, 2004). The financial healthcare burden of DFUs is therefore considerable.

It is widely accepted that delayed wound healing resulting from peripheral circulatory disorders is the critical pathomechanism in the development of diabetic ulcers (Forsythe & Hinchliffe, 2016). Wound healing occurs as a physiologic response to injury and involves neovascularization and angiogenesis (Hugo et al., 2016). Endothelial precursor cells (EPCs) have been found to play a remarkable part in the process of neovascularization and maintenance of endothelium homeostasis (Thal et al., 2012). These cells can be mobilized from the bone marrow and then participate in angiogenesis triggered by ischemia in a wound (Wang et al., 2018). Clinical evidence suggests that EPC transplantation has beneficial effects on wound rehabilitation in patients with ischemic limbs (Lara-Hernandez et al., 2010). Consequently, EPCs are a key part of the optimal curative response, but both the number and function of EPCs are impaired in diabetic patients (Wils et al., 2017). Allotransplantation of EPCs from healthy donors also faces the problem of immunological rejections (Tan et al., 2017) and the elevation of autologous EPC quantity and/or activity is therefore considered to be a promising therapeutic strategy for angiogenesis-related diseases.

Rosiglitazone (RSG) is a kind of peroxisome proliferator-activated receptor-gamma (PPAR-γ) agonist, commonly used to treat type 2 diabetes mellitus (T2DM), which could enhance insulin sensitivity (Hiatt et al., 2013). Several beneficial effects of RSG on EPCs have been convincingly described. *In vitro* findings support RSG's attenuation of EPC dysfunction and apoptosis, and the related signaling pathways are involved in ERK/MAPK, NF-κB, and Akt-eNOS of EPCs (Sheng et al., 2011; Chun et al., 2009). In addition, clinical research suggests that RSG treatment for 12 weeks improves EPC amounts and migratory ability in patients with

98 T2DM (Pistrosch et al., 2005). Nevertheless, the possible impact of PPAR-γ agonist RSG on

99 EPC behavior in wound healing in animals has not yet been described.

100 On the basis of existing evidence, we hypothesize that the beneficial effects of RSG extend to

101 EPC-mediated wound healing. To test this hypothesis, the present research focuses on

102 determining the influence of RSG on diabetes-induced wound healing and EPC function in

103 genetically diabetic *db/db* mice.

104

105

106

107

108

109

110

111

112

113

114

115

116

117

118

119

120

121

122

123

124

125

126

127

128

129

130

131

132

Materials & Methods

Animals. Six-week-old male C57BLKS/J *db/db* mice and male C57BL/6J mice were purchased from the Laboratory Animal Center of Zhejiang Province (Hangzhou, China) with experimental animal use license SYXK 2014-0008. All mice were housed in a 12 h light/dark cycle with an ambient temperature of 24 ± 2 ℃ and 50% humidity conditions. The mice had free access to water and standard chow. Animals used in this study received humane care in compliance with the National Institutes of Health Guide for the Care and Use of Laboratory Animals. The experimental protocols were approved by the Ethics Committee of Laboratory Animal Care and Welfare, Zhejiang Academy Medical Sciences, with the proved number 2018-141.

Experimental protocols. Male *db/db* mice with hyperglycemia were used as a T2DM animal model, and all mice began blood glucose monitoring at 8-week-old for 3 weeks to determine diabetes. Random blood glucose was determined with whole blood samples collected from the tail veins by a monitoring system (AB-101G, Maochang, Taiwan). Mice with random blood glucose greater than 300mg/dL were recognized as diabetes. A total of 32 diabetic mice were randomly divided into two groups at 11-week-old and treated with either RSG (16 mice, 20mg/kg/d, *i.g.*; Wang et al. 2017) or vehicle (16 mice, 0.5% CMC-Na, *i.g.*) for 28 days. The C57BL/6 mice were also randomly divided into a vehicle group (16 mice) and an RSG group (16 mice). At 15-week-old, 10 mice from each group were used for the wound closure experiment and six mice were anesthetized to harvest bone marrow-EPCs (BM-EPCs) (Figure 1A).

Evaluation of wound healing. Mice were anesthetized by intraperitoneal injection of ketamine (100 mg/kg). After being fixed on a bubble board and having hair removed from the dorsum, a 6 mm circle wound was made by punch biopsy (Han et al., 2017). The process of wound healing was monitored by pictures every 2 days until the wounds of the control mice completely healed. The areas of the wounds were evaluated by Image-Pro Plus software version 6.0 (Media Cybernetics, MD, USA) and the rate of wound closure was calculated.

Quantification of wound angiogenesis. Quantification of wound angiogenesis was conducted by CD31 (a platelet endothelial cell adhesion molecule) immunochemistry and hematoxylin staining (Han et al., 2017). Skin samples following the wound edges were harvested from the experimental mice on days 7 and 14. Collection samples were fixed in 4% paraformaldehyde for 10 h at room temperature and then embedded in paraffin for immunochemistry processing. Samples were cut into 5 μm thick sections, blocked with 5% serum (Chemicon International,

164   Inc., CA, USA) for 3 h, and then incubated with an anti-CD31antibody (1:500, cat. No. 550274;

165   BD Biosciences, CA, USA) for 1 h. The slides were subsequently incubated with a biotinylated

166   secondary antibody (1:800, cat. No. BA-9200; Vector Laboratories Ltd., Peterborough, UK) for

167   1 h. Finally, the slides were counterstained with hematoxylin for 2 min. The tubular structure that

168   was positive for CD31 was regarded as capillary, and the capillary numbers were analyzed.

169   Three sections of slides from each experimental mouse were evaluated under high-power fields

170   (magnification ×200) by a light microscope (Leica, Wezlar, Germany).

171   *Isolation of the BM-EPCs.* The BM-EPCs of the mice were isolated and cultured as described

172   previously (Xie et al., 2010). BM-EPCs were extracted from the tibias and femurs of mice and

173   suspended in endothelial growth medium-2 (Cambrex Corp., NJ, USA), containing 15% fetal

174   bovine serum (Gibco, Thermo Fisher Scientific, Inc.). Cells were plated into 6-well plates

175   (Coring, MA, USA) at 37℃ with 5% carbon dioxide (CO_2). After the cells were adhered to the

176   plates, non-adherent cells were removed and fresh medium was added to the adhered cells and

177   allowed to incubate for 3 days. BM-EPCs were used for function analysis and the supernatant

178   for ELISA quantification.

179   *Analysis of BM-EPC function.* Tube formation assay was performed to assess BM-EPC function

180   as described previously (Yu et al., 2016). Before starting the experiment, a 96-well plate was

181   pre-treated with 50 μl/well of growth factor induced Matrigel (BD Biosciences) for 30 min. Cells

182   were seeded in the pre-treated plate at a concentration of 5×10^5/ml. After 6 h of incubation,

183   images of the formation tubes were captured under high-power fields (magnification ×50) using

184   a light microscope. The numbers of tubes were then calculated.

185   The migratory ability assay was also used to evaluate EPC function as previously described (Yu

186   et al., 2016). A 24-well transwell plate with modified Boyden chamber (pore size 8 μm; Coring

187   Transwell, MA, USA) was used in this assay. A total of 50,000 cells were plated to the upper

188   chamber with 8 μm pores on the polycarbonate membrane, and vascular endothelial growth

189   factor (VEGF; 50ng/ml; cat. No. V4512; Sigma-Aldrich, Darmstadt, Germany) was added to the

190   medium in the lower chamber. After incubation at 37℃ with 5% CO_2 for 24 h, the cells were

191   fixed in 2% paraformaldehyde for 15 min and stained using Hoechst 33258 (10 μg/ml; cat. No.

192   C1011; Beyotime, Shanghai, China). The migration of cells from the upper chamber to the lower

193   was measured under a fluorescence microscope. The number of migrating EPCs was counted.

194   *Determination of VEGF protein.* The supernatant of the BM-EPCs in *db/db* mice after treatment

195   with RSG was collected and the concentrations of VEGF were detected by an ELISA Kit (R&D

196   systems, MN, USA) according to the manufacturer's instruction.

197   *Detection of stromal cell derived factor -1α (SDF-1α) protein.* Blood was harvested from *db/db*

198   mice; the serum concentrations of SDF-1α protein were detected using an ELISA Kit (R&D

199   systems, MN, USA). Measurements were performed according to the manufacturer's instruction.

200   *Assessment of BM-EPC insulin signaling.* AKT activity was used to evaluate insulin signaling

201   according to previously describe (Desouza et al., 2011). BM-EPCs from the C57BL/6 mice and

202   the *db/db* mice were seeded onto the 96-well plate. The cells were treated with or without 1

203   μmol/L insulin for 1 h to induce the insulin signaling pathway. Then, the phosphorylated AKT

204   and the total AKT of cells was determined by the ELISA Kit (R&D systems, MN, USA)

205   according to manufacturer's instruction. Phosphorylated-to-total AKT ratios were calculated.

206   *In Vitro Assay.* BM-EPCs were obtained from the C57BL/6 mice and cultured *in vitro*. After

207   seven days of cultivation, the medium was replaced with high glucose (HG; 33 mM) medium,

208   HG medium containing RSG (10 nM), or HG medium containing both RSG (10 nM) and avastin

209   (a VEGF inhibitor; 25 μg/ml; Merz et al., 2018) for 24 h. The effects of RSG on HG-induced

210   EPC activity and tube formation function were determined. Activation of BM-EPCs was

211   determined by cell counting kit -8 (CCK-8; Dojindo Laboratory, Kumamoto, Japan) according to

212   the manufacturer's instruction. EPCs were washed with phosphate buffer (PBS) and then

213   incubated with 10 μl CCK-8 solution for 2 h at 37℃. The optical density was measured at 450

214   nm using a Microplate Reader (Bio-Rad, Hercules, CA, USA).

215   *Statistical analysis.* All data is presented as mean ± standard error of the mean (SEM). Statistical

216   significance was determined with one-way analysis of variance (ANOVA) followed by the

217   Newman-Keuls multiple comparison test of using GraphPad Prism Software version 6. A value

218   for *P* less than 0.05 was considered to be a statistically significant difference.

219

220

221

222

223

224

225

Results

Effect of rosiglitazone on blood glucose, serum insulin level, and body weight in db/db mice. In *db/db* diabetic mice, the blood glucose level was greatly elevated when compared to the control group (426.4 ± 1.5 *vs* 112.1 ± 1.5 mg/dL, $P < 0.05$; Figure 1B). RSG therapy for 4 weeks significantly decreased the blood glucose concentration and increased serum insulin level compared with *db/db* mice (Figure 1C : 350.2 ± 31.1 *vs* 451.6 ± 26.8 mg/dL, $P < 0.05$; Figure 1D: 4.3 ± 0.2 *vs* 3.5 ± 0.3 μIU/ml, $P < 0.05$). In accordance with the blood glucose improvement, there was also a significant decrease in body weight in the RSG pre-treatment *db/db* mice (Figure 1E).

Rosiglitazone accelerated wound closure and wound angiogenesis in db/db mice. To examine the role of RSG treatment on wound healing in *db/db* diabetic mice, the wound area was measured on alternate days until day 14. A significant slowing of wound healing was shown in *db/db* mice when compared to the control group, and RSG greatly accelerated the wound healing in diabetic mice ($P< 0.05$; Figure 2A-U). On day 14 post injury, histological assessment showed that the RSG-treated *db/db* wounds had thicker neo-epidermal sheets and more granulation formation than *db/db* diabetic mice (Figure 3A-B).

To further assess the effect of RSG on neovascularization, the number of CD31-positive stains indicating the tubular structures, was counted in the wound area and surrounding skin. Figures 3C-J show the deteriorated capillary formation on days 7 and 14, respectively, in *db/db* mice, compared with the control group. RSG significantly alleviated capillary formation on both day 7 and day 14 in *db/db* mice ($P < 0.05$; Figure 3C-J) suggesting that RSG therapy accelerates wound healing and enhances wound vascularity in diabetic mice.

Rosiglitazone alleviated BM-EPC function in db/db mice. Next, we explored the mechanism of RSG in accelerating wound healing using the tube formation assay and migration assay. Impaired BM-EPC function was seen in the diabetic mice when compared to the control group. As expected, administration of RSG attenuated the decline of BM-EPC function in *db/db* mice, reflected by tube formation (21.0 ± 1.5 *vs* 12.7 ± 1.1 $P < 0.05$; Figure 4A-D, I) and migration ability ($55.3\% \pm 2.5\%$ *vs* $36.2\% \pm 3.3\%$ $P < 0.05$; Figure 4E-H, J).

Rosiglitazone elevated the level of SDF-1α and VEGF protein in db/db mice. Reduced SDF-1αand VEGF levels have been shown to be involved in diabetes-induced refractory wounds and impaired homing of EPCs. The levels of SDF-1α and VEGF protein were therefore measured in

257   the diabetic mice. It was found that the level of SDF-1α was significantly decreased in *db/db*

258   mice compared with the control group (2.6 ± 0.3 *vs* 4.6 ± 0.3 ng/mL $P < 0.05$; Figure 5A). RSG-

259   treated mice exhibited markedly increased levels of SDF-1α (3.4 ± 0.1 *vs* 2.6 ± 0.3 ng/mL, $P <$

260   0.05; Figure 5A). VEGF levels were significantly lower in the *db/db* mice than in the control

261   group (423.7 ± 19.6 *vs* 614.0 ± 27.1 pg/mL $P < 0.05$; Figure 5B), and RSG treatment greatly

262   prevented this decrease (497.3 ± 16.5 *vs* 423.7 ± 19.6 pg/mL $P < 0.05$; Figure 5B).

263   *Rosiglitazone increased insulin signaling in BM-EPCs of db/db mice.* Clinical researches have

264   reported that dysfunction of EPCs is positively correlated with insulin resistance in patients with

265   T2DM (Dei Cas et al., 2011; Cubbon et al., 2007). Here we determined whether DM

266   environment induces insulin signaling defects in EPCs and whether treatment with RSG reduces

267   the defects. To test this hypothesis, we used BM-EPCs stimulated by insulin and measured AKT

268   activity. As illustrated in Figure 5C, BM-EPCs obtained from the *db/db* mice were markedly

269   insulin resistant as measured by phosphorylated-to-total AKT ratio compared with BM-EPCs

270   from the C57BL/6 mice (2.2 ± 0.04 *vs* 5.6 ± 0.2 $P < 0.05$). AKT activity was significantly up-

271   regulated in BM-EPCs from RSG-treated *db/db* mice when compared with the vehicle treated

272   *db/db* mice (4.2 ± 0.3 *vs* 2.2 ± 0.04 $P < 0.05$; Figure 5C).

273   *Avastin prevented the action of RSG in EPCs in vitro.* High glucose is commonly used as an EPC

274   injury model *in vitro*. To clarify the role of VEGF in EPC function induced by high glucose,

275   avastin a VEGF inhibitor was used. The cell viability and capacity for tube formation of BM-

276   EPCs were greatly impaired by high glucose. RSG (10 nM) treatment significantly increased cell

277   viability (85.4 ± 1.9 *vs* 73.4 ± 2.7%, $P < 0.05$; Figure 6A) and improved the impaired EPC

278   function (30.2 ± 1.4 *vs* 19.8 ± 1.5, $P < 0.05$; Figure 6B-F). Inhibition of VEGF levels abolished

279   the enhanced EPC viability and function mediated by RSG (EPC viability: 73.3 ± 2.6 *vs* 85.4 ±

280   1.9%, $P < 0.05$; Figure 6A; Tube number: 22.0 ± 1.7 *vs* 30.2 ± 1.4, $P < 0.05$; Figure 6B-F).

281

282

283

284

285

286

287

Discussion

288 **Discussion**

289 Three principal findings arose from this study. First, administration of RSG accelerated wound

290 healing and improved angiogenesis in *db/db* diabetic mice. Second, we found that RSG

291 alleviated the impaired BM-EPC capacity and insulin resistance in *db/db* mice. Third, we

292 showed that RSG elevated VEGF and SDF-1α levels in diabetic mice, and inhibition of VEGF

293 could abolish the improved EPC viability and tube formation function mediated by RSG *in vitro*

294 .

295   D*b/db* mice have become a well-established animal model for T2DM that has been widely used

296 in animal experiments. As a consequence of gene mutation of the leptin receptor, *db/db* mice

297 exhibit spontaneous glucose metabolic disorder, which is similar to the clinical symptoms of

298 adult-onset T2DM. There is strong evidence that suggests that sustained hyperglycemia cannot

299 occur until 8 weeks old (Bao et al., 2016), so 8-week-old mice were therefore selected for this

300 study, and stable high blood glucose was shown from week 8 to week 10 (Figure 2A). The

301 results suggest that a typically diabetic animal model was established.

302   Wound healing following tissue injury occurs as a cellular response, which involves activation

303 of endothelial cells and the release of numerous signaling molecules (Longmate et al., 2017).

304 Individuals with DM and associated high blood glucose suffer wound healing illness and

305 subsequent complications, such as peripheral vascular disorder and lower limb amputation (Brem

306 et al., 2007). It has been long understood that angiogenesis plays an important role in the process

307 of wound healing at many stages. Physiologically, angiogenesis takes part in the formation of

308 new blood vessels, and this is involved in endothelial cell repair and especially BM-EPC

309 mobilization (Saboo et al., 2016). CD31, also called platelet endothelial cell adhesion molecule -

310 1 (PECAM-1), is a marker that indicates existing endothelial cells and vascular formation in

311 immunohistochemical assay (Lertkiatmongkol et al., 2016). Consistent with previous studies

312 (Han et al., 2017), we found that angiogenesis capacity at the wound sites, as indicated by CD31

313 staining, was impaired in the *db/db* diabetic mice compared to the non-diabetic subjects.

314 However, the underlying mechanism of angiogenesis under the pathologic condition of DM

315 remains a significant aspect yet to be explained.

316   EPCs have previously been reported to have a close relationship with neovascularization in

317 response to complicated diabetic wound. EPCs in bone marrow respond to ischemia with

318 chemokine factors, which result in the homing of the impaired site, where they are implicated in

319   vascular repair and new vessel formation as mature endothelial cells (Gao et al., 2008).
320   Unexpectedly, studies have indicated that the mobilization ability of EPCs from bone marrow to
321   peripheral blood declines much more in diabetic patients than in normal individuals, resulting in
322   decreased numbers of circulating EPCs (Falay & Aktas, 2016). In line with these results, we
323   have found that the activity and total numbers of EPCs were reduced both in *db/db* mice and in
324   mice exposed to streptozocin (Han et al., 2017; Yu et al., 2016). RSG, a PPAR-γ agonist family
325   member, is approved for use as a single drug or in combination with metformin therapy for
326   T2DM. The hypoglycemic mechanism of RSG is recognized as a mediator of increased insulin
327   sensitivity in muscles and adipose tissues (Kolak et al., 2007). Previous studies have reported
328   that RSG could reduce EPC apoptosis and improve impaired EPC-induced angiogenesis,
329   suggesting that RSG has beneficial effects on EPC biology (Verma et al., 2004; Haberzettl et al.,
330   2016). Clinical studies have also demonstrated that RSG contributes to improved EPC numbers
331   and migratory function in T2DM patients (Pistrosch et al., 2005), but the associated mechanisms
332   have been largely unclear. In the current study, we found that administration of RSG accelerated
333   wound closure and increased capillary density, accompanied by improvement of the tube
334   formation and migratory activity of EPCs in *db/db* mice. These results imply that the efficacy of
335   RSG in wound healing was potentially related to regulation of EPC dysfunction under diabetic
336   pathology conditions. Furthermore, in human, dysfunction of EPCs is also in the presence of the
337   insulin resistance syndrome (Desouza et al., 2011). Our results showed that RSG ameliorated
338   insulin signaling defects in BM-EPCs of *db/db* mice.
339   VEGF has been shown to be a pivotal player in promoting endothelial cell migration (Morales-
340   Ruiz et al., 2000; Dimmeler et al., 2000) and EPC-mediated angiogenesis. Blood VEGF levels
341   are indeed positively associated with good prognosis for wounds in diabetes. For RSG, there is
342   controversial data regarding the influence on VEGF expression. On one hand, Ku et al. (2017)
343   reported that RSG might promote neovascularization and vascular permeability by inducing
344   VEGF expression, and myofibroblasts exhibit an up-regulation of VEGF-dependent PPAR-γ
345   inhibition (Chintalgattu et al., 2007). On the other hand, RSG failed to increase VEGF level in
346   cultured mesangial cells under high glucose conditions (Whiteside et al., 2009) and inhibited
347   biosynthesis of VEGF in keratinocytes (Schiefelbein et al., 2008). In the current study, RSG
348   increased VEGF expression in BM-EPCs of diabetic mice. Inhibition of VEGF abolished the
349   enhanced EPC viability and tube formation mediated by RSG. Furthermore, EPC recruitment to

350 the site of the wound depends on up-regulation of the SDF-1α. Preclinical studies have
351 demonstrated a decrease in SDF-1α at wound sites in diabetic mice and this decrease is
352 responsible for reduced EPC homing (Gallagher et al., 2007). The present study determined that
353 treatment with RSG significantly up-regulated SDF-1α levels accompanying accelerated wound
354 healing in *db/db* mice.

355 Actually, we did have some limitations for this study. In particular, the mice dorsal wounds
356 exhibit furious contraction during healing, which is different from the process in human wounds,
357 where heal is through granulation and reepithelialization (Konop et al., 2017). We did not use the
358 wound splinting model to prevent skin contraction (Konop et al., 2017; Wang et al., 2013), even
359 our wound model was used as previously reported (Han et al., 2017; Yu et al., 2016; Li et al.,
360 2016).

361 ## Conclusion

362 We demonstrated that RSG therapy protects against diabetes-induced wound healing delay,
363 angiogenesis disorder, and EPC dysfunction in *db/db* diabetic mice. Administration of RSG
364 accelerated wound closure, which was partially correlated with an amelioration of EPC function
365 through activation of VEGF/SDF-1α and insulin signaling. These results suggest that RSG may
366 be a promising drug for local wound closure of DFUs, given its well-established
367 pharmacological action of glucose-lowering.

368
369

370 ## Funds

371 This study was supported by the Natural Science Foundation of Zhejiang (Grants
372 LGJ18H310002 and LQY19H090001), National Natural Science Foundation of China (No.
373 31870080 and 31900381), the Youth start-up fund of Second Military Medical University (Grant
374 No. 2018QN13), Innovation Training Program of Anhui (No. 201810368117).

375
376
377
378
379
380
381

382

References

Abbott CA, Carrington AL, Ashe H, Bath S, Every LC, Griffiths J, Hann AW, Hussein A, Jackson N, Johnson KE, Ryder CH, Torkington R, Van Ross ER, Whalley AM, Widdows P, Williamson S, Boulton AJ. 2002. The North West Diabetes Foot Care Study: incidence of, and risk factors for, new diabetic foot ulceration in a community-based patient cohort. *Diabetic Med* **19(5)**:377–384.

Bao Q, Shen X, Qian L, Gong C, Nie M, Dong Y. 2016. Anti-diabetic activities of catalpol in db/db mice. *Korean J Physiol Pharmacol* **20(2):** 153-160 DOI 10.4196/kjpp.2016.20.2.153.

Brem H, Tomic-Canic M. 2007. Cellular and molecular basis of wound healing in diabetes. *J Clin Invest* **117(5)**:1219-22 DOI 10.1172/JCI32169.

Chintalgattu V, Harris GS, Akula SM, Katwa LC. 2007. PPAR-gamma agonists induce the expression of VEGF and its receptors in cultured cardiac myofibroblasts. *Cardiovasc Res* **74(1):**140–50 DOI 10.1016/j.cardiores.2007.01.010.

Chun Liang, Yusheng Ren, Hongbin Tan, Zhiqing He, Qijun Jiang, Jianxiang Wu, Yi Zhen, Min Fan, Zonggui Wu. 2009. Rosiglitazone via upregulation of Akt/eNOS pathways attenuates dysfunction of endothelial progenitor cells, induced by advanced glycation end products. *British Journal of Pharmacology* **158(8):**1865-73 DOI 10.1111/j.1476-5381.2009.00450.x.

Cubbon RM, Rajwani A, Wheatcroft SB. 2007. The impact of insulin resistance on endothelial function, progenitor cells and repair. *Diab Vasc Dis Res* **4(2)**:103–111 DOI 10.3132/dvdr.2007.027.

Dei Cas A, Spigoni V, Ardigò D, Pedrazzi G, Franzini L, Derlindati E, Urbani S, Monti L, Gnudi L, Zavaroni I. 2011. Reduced circulating endothelial progenitor cell number in healthy young adult hyperinsulinemic men. *Nutr Metab Cardiovasc Dis* **21(7)**:512-7 DOI 10.1016/j.numecd.2009.11.011.

Desouza CV, Hamel FG, Bidasee K, O'Connell K. 2011. Role of Inflammation and Insulin Resistance in Endothelial Progenitor Cell Dysfunction. *Diabetes* **60(4)**:1286-94. DOI 10.2337/db10-0875.

411 **Dimmeler S, Dernbach E, Zeiher AM. 2000.** Phosphorylation of the endothelial nitric oxide
412   synthase at ser-1177 is required for VEGF-induced endothelial cell migration. *FEBS Lett*
413   **477(3):**258–62.

414 **Evran Olgun M, Altuntaş SC, Sert M, Tetiker T. 2019.** Anemia in Patients with Diabetic Foot
415   Ulcer: Effects on Diabetic Microvascular Complications and Related Conditions. *Endocr*
416   *Metab Immune Disord Drug Targets* DOI 10.2174/1871530319666190111121913.

417 **Falay M, Aktas S. 2016.** Endothelial Progenitor Cells (EPC) Count by Multicolor Flow
418   Cytometry in Healthy Individuals and Diabetes Mellitus (DM) Patients. *Clin Lab* **62(11):**
419   2161-2166 DOI 10.7754/Clin.Lab.2016.160402.

420 **Forsythe RO, Hinchliffe RJ. 2016.** Assessment of foot perfusion in patients with a diabetic foot
421   ulcer. *Diabetes Metab Res Rev* **32 (Suppl 1)**:232-8 DOI 10.1002/dmrr.2756.

422 **Gallagher KA, Liu ZJ, Xiao M, Chen H, Goldstein LJ, Buerk DG, Nedeau A, Thom SR,**
423   **Velazquez OC. 2007.** Diabetic impairments in NO-mediated endothelial progenitor cell
424   mobilization and homing are reversed by hyperoxia and SDF-1 alpha. *J Clin Invest*
425   **117(5):**1249–1259 DOI 10.1172/JCI29710.

426 **Gao D, Nolan DJ, Mellick AS, Bambino K, McDonnell K, Mittal V. 2008.** Endothelial
427   progenitor cells control the angiogenic switch in mouse lung metastasis. *Science*
428   **319(5860):**195-8 DOI 10.1126/science.1150224.

429 **Ku YH, Cho BJ, Kim MJ, Lim S, Park YJ, Jang HC, Choi SH. 2017.** Rosiglitazone increases
430   endothelial cell migration and vascular permeability through Akt phosphorylation. *BMC*
431   *Pharmacol Toxicol* **18(1):**62 DOI 10.1186/s40360-017-0169-y.

432 **Haberzettl P, McCracken JP, Bhatnagar A, Conklin DJ. 2016.** Insulin sensitizers prevent
433   fine particulate matter-induced vascular insulin resistance and changes in endothelial
434   progenitor cell homeostasis. *Am J Physiol Heart Circ Physiol* **310(11):**H1423-38 DOI
435   10.1152/ajpheart.00369.

436 **Han X, Deng Y, Yu J, Sun Y, Ren G, Cai J, Zhu J, Jiang G. 2017.** Acarbose Accelerates
437   Wound Healing via Akt/eNOS Signaling in db/db Mice. *Oxid Med Cell Longev*
438   **2017:**7809581 DOI 10.1155/2017/7809581.

439 **Han X, Tao Y, Deng Y, Yu J, Sun Y, Jiang G. 2017.** Metformin accelerates wound healing in
440   type 2 diabetic db/db mice. *Mol Med Rep* **16(6):**8691-8698 DOI 10.3892/mmr.2017.7707.

441 **Hiatt WR, Kaul S, Smith RJ. 2013.** The cardiovascular safety of diabetes drugs--insights from
442   the rosiglitazone experience. *N Engl J Med* **369(14)**:1285-7 DOI 10.1056/NEJMp1309610.

443 **Hugo W, Zaretsky JM, Sun L, Song C, Moreno BH, Hu-Lieskovan S, Berent-Maoz B, Pang**
444   **J, Chmielowski B, Cherry G, Seja E, Lomeli S, Kong X, Kelley MC, Sosman JA,**
445   **Johnson DB, Ribas A, Lo RS. 2016.** Genomic and Transcriptomic Features of Response to
446   Anti-PD-1 Therapy in Metastatic Melanoma. *Cell* **165(1)**:35-44 DOI
447   10.1016/j.cell.2016.02.065.

448 **Kolak M, Yki-Jarvinen H, Kannisto K, Tiikkainen M, Hamsten A, Eriksson P, Fisher RM.**
449   **2007.** Effects of chronic rosiglitazone therapy on gene expression in human adipose tissue in
450   vivo in patients with type 2 diabetes. *J Clin Endocrinol Metab* **92(2):**720–724 DOI
451   10.1210/jc.2006-1465.

452 **Konop M, Sulejczak D, Czuwara J, Kosson P, Misicka A, Lipkowski AW, Rudnicka L.**
453   **2017.** The role of allogenic keratin‐derived dressing in wound healing in a mouse model.
454   *Wound Repair Regen* **25(1)**:62-74 DOI 10.1111/wrr.12500.

455 **Lara-Hernandez R, Lozano-Vilardell P, Blanes P, Torreguitart-Mirada N, Galmés A,**
456   **Besalduch J. 2010.** Safety and efficacy of therapeutic angiogenesis as a novel treatment in
457   patients with critical limb ischemia. *Ann Vasc Surg* **24(2)**:287-94 DOI 10.1016/j.avsg.

458 **Lertkiatmongkol P, Liao D, Mei H, Hu Y, Newman PJ. 2016.** Endothelial functions of
459   platelet/endothelial cell adhesion molecule-1 (CD31). *Curr Opin Hematol* **23(3):**253-9 DOI
460   10.1097/MOH.0000000000000239.

461 **Li ZP, Xin RJ, Yang H, Jiang GJ, Deng YP, Li DJ, Shen FM. 2016.** Diazoxide accelerates
462   wound healing by improving EPC function. *Front Biosci (Landmark Ed)* **21**:1039-51.

463 **Longmate WM, Lyons SP, Chittur SV, Pumiglia KM, Van De Water L, DiPersio CM.**
464   **2017.** Suppression of integrin α3β1 by α9β1 in the epidermis controls the paracrine resolution
465   of wound angiogenesis. *J Cell Biol* **216(5):**1473-1488 DOI 10.1083/jcb.201510042.

466 Merz PR, Röckel N, Ballikaya S, Auffarth GU, Schmack I. 2018. Effects of ranibizumab
467   (Lucentis®) and bevacizumab (Avastin®) on human corneal endothelial cells. *BMC*
468   *Ophthalmol* **18(1)**:316 DOI 10.1186/s12886-018-0978-9.

469 **Morales-Ruiz M, Fulton D, Sowa G, Languino LR, Fujio Y, Walsh K, Sessa WC. 2000.**
470   Vascular endothelial growth factor-stimulated actin reorganization and migration of
471   endothelial cells is regulated via the serine/threonine kinase Akt. *Circ Res* **86(8):**892–6.

472 **Pistrosch F, Herbrig K, Oelschlaegel U, Richter S, Passauer J, Fischer S, Gross P. 2005.**

473   PPARγ-agonist rosiglitazone increases number and migratory activity of cultured endothelial

474   progenitor cells. *Atherosclerosis* **183(1):**163-7 DOI 10.1016/j.atherosclerosis.2005.03.039.

475 **Saboo A, Rathnayake A, Vangaveti VN, Malabu UH. 2016.** Wound healing effects of

476   dipeptidyl peptidase-4 inhibitors: An emerging concept in management of diabetic foot ulcer-

477   A review. *Diabetes Metab Syndr* **10(2):**113-9 DOI 10.1016/j.dsx.2015.04.006.

478 **Schiefelbein D, Seitz O, Goren I, Dissmann JP, Schmidt H, Bachmann M, Sader R,**

479   **Geisslinger G, Pfeilschifter J, Frank S. 2008.** Keratinocyte-derived vascular endothelial

480   growth factor biosynthesis represents a pleiotropic side effect of peroxisome proliferator-

481   activated receptor-gamma agonist troglitazone but not rosiglitazone and involves activation of

482   p38 mitogen-activated protein kinase: implications for diabetes-impaired skin repair. *Mol*

483   *Pharmacol* **74(4):**952–63 DOI 10.1124/mol.108.049395.

484 **Shengjie Xu, Yanbo Zhao, Lu Yu, Xiaohua Shen, Fang Ding, Guosheng Fu. 2011.**

485   Rosiglitazone Attenuates Endothelial Progenitor Cell Apoptosis Induced by TNF-α via

486   ERK/MAPK and NF-κB Signal Pathways. *J Pharmacol Sci* **117(4)**: 265 – 274.

487 **Tan K, Zheng K, Li D, Lu H, Wang S, Sun X. 2017.** Impact of adipose tissue or umbilical

488   cord derived mesenchymal stem cells on the immunogenicity of human cord blood derived

489   endothelial progenitor cells. *PLoS One* **12(5)**:e0178624 DOI 10.1371/journal.pone.0178624.

490 **Tennvall GR, Apelqvist J. 2004.** Health-economic consequences of diabetic foot lesions. *Clin*

491   *Infect Dis* **39(Suppl 2)**: S132–9 DOI 10.1086/383275.

492 **Thal MA, Krishnamurthy P, Mackie AR, Hoxha E, Lambers E, Verma S, Ramirez V, Qin**

493   **G, Losordo DW, Kishore R. 2012.** Enhanced angiogenic and cardiomyocyte differentiation

494   capacity of epigenetically reprogrammed mouse and human endothelial progenitor cells

495   augments their efficacy for ischemic myocardial repair. *Circ Res* **111(2)**:180-90 DOI

496   10.1161/CIRCRESAHA.112.270462.

497 **Verma S, Kuliszewski MA, Li SH, Szmitko PE, Zucco L, Wang CH, Badiwala MV, Mickle**

498   **DA, Weisel RD, Fedak PW, Stewart DJ, Kutryk MJ. 2004.** C-Reactive Protein Attenuates

499   Endothelial Progenitor Cell Survival, Differentiation, and Function Further Evidence of a

500   Mechanistic Link Between C-Reactive Protein and Cardiovascular Disease. *Circulation*

501   **109(17):**2058-67 DOI 10.1161/01.CIR.0000127577.63323.24.

502 **Wan H, Wang Y, Zhang K, Chen Y, Fang S, Zhang W, Wang C, Li Q, Xia F, Wang N, Lu**
503   **Y. 2019.** Associations between vitamin D and microvascular complications in middle-aged
504   and elderly diabetic patients. *Endocr Pract* DOI 10.4158/EP-2019-0015.

505 **Wang C, Mao C, Lou Y, Xu J, Wang Q, Zhang Z, Tang Q, Zhang X, Xu H, Feng Y. 2018.**
506   Monotropein promotes angiogenesis and inhibits oxidative stress-induced autophagy in
507   endothelial progenitor cells to accelerate wound healing. *J Cell Mol Med* **22(3)**:1583-1600
508   DOI 10.1111/jcmm.13434.

509 **Wang JX, Zhang C, Fu L, Zhang DG, Wang BW, Zhang ZH, Chen YH, Lu Y, Chen X, Xu**
510   **DX. 2017.** Protective effect of rosiglitazone against acetaminophen-induced acute liver injury
511   is associated with down-regulation of hepatic NADPH oxidases. *Toxicol Lett* **265**:38-46 DOI
512   10.1016/j.toxlet.2016.11.012.

513 **Wang X, Ge J, Tredget EE, Wu Y. 2013.** The mouse excisional wound splinting model,
514   including applications for stem cell transplantation. *Nat Protoc* **8(2)**:302-9 DOI
515   10.1038/nprot.2013.002.

516 **Whiteside C, Wang H, Xia L, Munk S, Goldberg HJ, Fantus IG. 2009.** Rosiglitazone
517   prevents high glucose-induced vascular endothelial growth factor and collagen IV expression
518   in cultured mesangial cells. *Exp Diabetes Res* **2009**:910783 DOI 10.1155/2009/910783.

519 **Wils J, Favre J, Bellien J. 2017.** Modulating putative endothelial progenitor cells for the
520   treatment of endothelial dysfunction and cardiovascular complications in diabetes. *Pharmacol*
521   *Ther* **170**:98-115 DOI 10.1016/j.pharmthera.2016.10.014.

522 **Xie HH, Zhou S, Chen DD, Channon KM, Su DF, Chen AF. 2010.** GTP cyclohydrolase
523   I/BH4 pathway protects EPCs via suppressing oxidative stress and thrombospondin-1 in salt-
524   sensitive   hypertension.   *Hypertension*   **56(6):**1137-44   DOI
525   10.1161/HYPERTENSIONAHA.110.160622.

526 **Yu JW, Deng YP, Han X, Ren GF, Cai J, Jiang GJ. 2016.** Metformin improves the
527 angiogenic functions of endothelial progenitor cells via activating AMPK/eNOS pathway in
528 diabetic mice. *Cardiovasc Diabetol* **15:**88 DOI 10.1186/s12933-016-0408-3.

529
530
531
532
533

534

535

536

537 Figure 1. Illustration of experimental schedule and establishment of *db/db* diabetic mice model. (A) All

538 mice at 8-week-old began blood glucose monitoring for 3 weeks to determine diabetes. *Db/db* mice were

539 treated with rosiglitazone (20mg/kg/d × 28d, *i.g.*) or vehicle at 11-week-old for consecutive 4 weeks, and

540 C57BL/6 mice also received RSG or vehicle. At 15-week-old, mice were further divided into 2 cohorts:

541 wound closure creation and BM-EPC harvest. (B) Significant elevation of the blood glucose was shown

542 in *db/db* mice compared with control group. RSG treatment greatly decreased the blood glucose (C),

543 increased the serum insulin levels (D) and lighten the body weight in *db/db* mice (E). Values are mean ±

544 SEM, (n=6 per group). *P <0.05 *vs.* Control; #P <0.05 *vs. db/db*. RSG, rosiglitazone.

545

546 Figure 2. Rosiglitazone administration accelerated wound closure in *db/db* diabetic mice. After 4 weeks

547 treated with RSG, *db/db* mice were produced a 6 mm circle wound on the dorsa by a punch biopsy and

548 then pictures of the wound were taken every 2 days until day 14. RSG treatment accelerated wound

549 closure in *db/db* mice. Representative pictures of wound closure on day 0, day 4, day8, day12 and day 14

550 (A-T) and quantitative analysis (U). Values are mean ± SEM, (n=5 per group). *P <0.05 *vs.* Control; #P

551 <0.05 *vs. db/db*. RSG, rosiglitazone.

552

553 Figure 3. Rosiglitazone administration increased wound angiogenesis in *db/db* diabetic mice. In *db/db*

554 mice, after wound closures were made, skins around the wound were collected and angiogenesis was

555 evaluated on days 7 and 14. Representative pictures of tissue destruction of wounds (A, B) and CD31

556 staining (C-H). Quantitative study on day 7 (I) and day 14 (J). Red arrows point out CD31-positive

557 capillaries (200×; scale bar, 50μm). Values are mean ± SEM, (n=5 per group). *P <0.05 *vs.* Control; #P

558 <0.05 *vs. db/db*. (&) Epidermis, (&&) dermis and (&&&) subcutis indicated. RSG, rosiglitazone. hpf,

559 high power field.

560

561 Figure 4. Rosiglitazone administration improved BM-EPC function in *db/db* diabetic mice. In *db/db* mice,

562 BM-EPCs were isolated and cultured after 4 weeks RSG therapy. BM-EPC function was estimated by

563 tube formation assay and migration assay. RSG treatment elevated tube formation ability (A-D, I) and

564 migration ability (E-H, J) of BM-EPCs. A: 50×; scale bar, 100μm; B: 100×; scale bar, 100μm. Values are

565 mean ± SEM, (n=6 per group). *P <0.05 *vs.* Control; #P <0.05 *vs. db/db*. RSG, rosiglitazone. lpf, low

566 power field.

567

568   Figure 5. Rosiglitazone administration increases the levels of VEGF and SDF-1α protein and improved

569   insulin resistant in *db/db* mice. (A) Effect of RSG treatment on SDF-1α protein levels in serum of the

570   *db/db* mice. (B) ELISA analyses of VEGF levels in supernatant of BM-EPCs. (C) BM-EPCs treated with

571   or without 1 μmol/L insulin for 1 h, and concentrations of phosphorylated AKT and total AKT were

572   determined by the ELISA kit. Values are mean ± SEM, (A, B: n=6; C: n=5 per group). A, B: $^{*}P$ <0.05

573   *vs.* Control; A, B: $^{\#}P$ <0.05 *vs. db/db*. RSG, rosiglitazone.

574

575   Figure 6. VEGF inhibitor avastin prevented the role of RSG in BM-EPCs induced by high glucose. (A)

576   BM-EPCs exposed to 33 mmol/L glucose with or without RSG (10 nM) and VEGF inhibitor Avastin (25

577   μg/ml) for 24 h. CCK-8 detected EPC viability *in vitro*. (B-F) Avastin abolished the elevated tube

578   formation ability by RSG (C-F: 50×; scale bar, 100μm). Values are mean ± SEM, (n=6 per group). RSG,

579   rosiglitazone. HG, high glucose.

Figure 1

Illustration of experimental schedule and establishment of *db/db* diabetic mice model

(A) All mice at 8-week-old began blood glucose monitoring for 3 weeks to determine diabetes. *Db/db* mice were treated with rosiglitazone (20mg/kg/d × 28d, *i.g.*) or vehicle at 11-week-old for consecutive 4 weeks, and C57BL/6 mice also received RSG or vehicle. At 15-week-old, mice were further divided into 2 cohorts: wound closure creation and BM-EPC harvest. (B) Significant elevation of the blood glucose was shown in *db/db* mice compared with control group. RSG treatment greatly decreased the blood glucose (C), increased the serum insulin levels (D) and lighten the body weight in *db/db* mice (E). Values are mean ± SEM, (n=6 per group). [*]P <0.05 *vs.* Control; [#]P <0.05 *vs. db/db*. RSG, rosiglitazone.
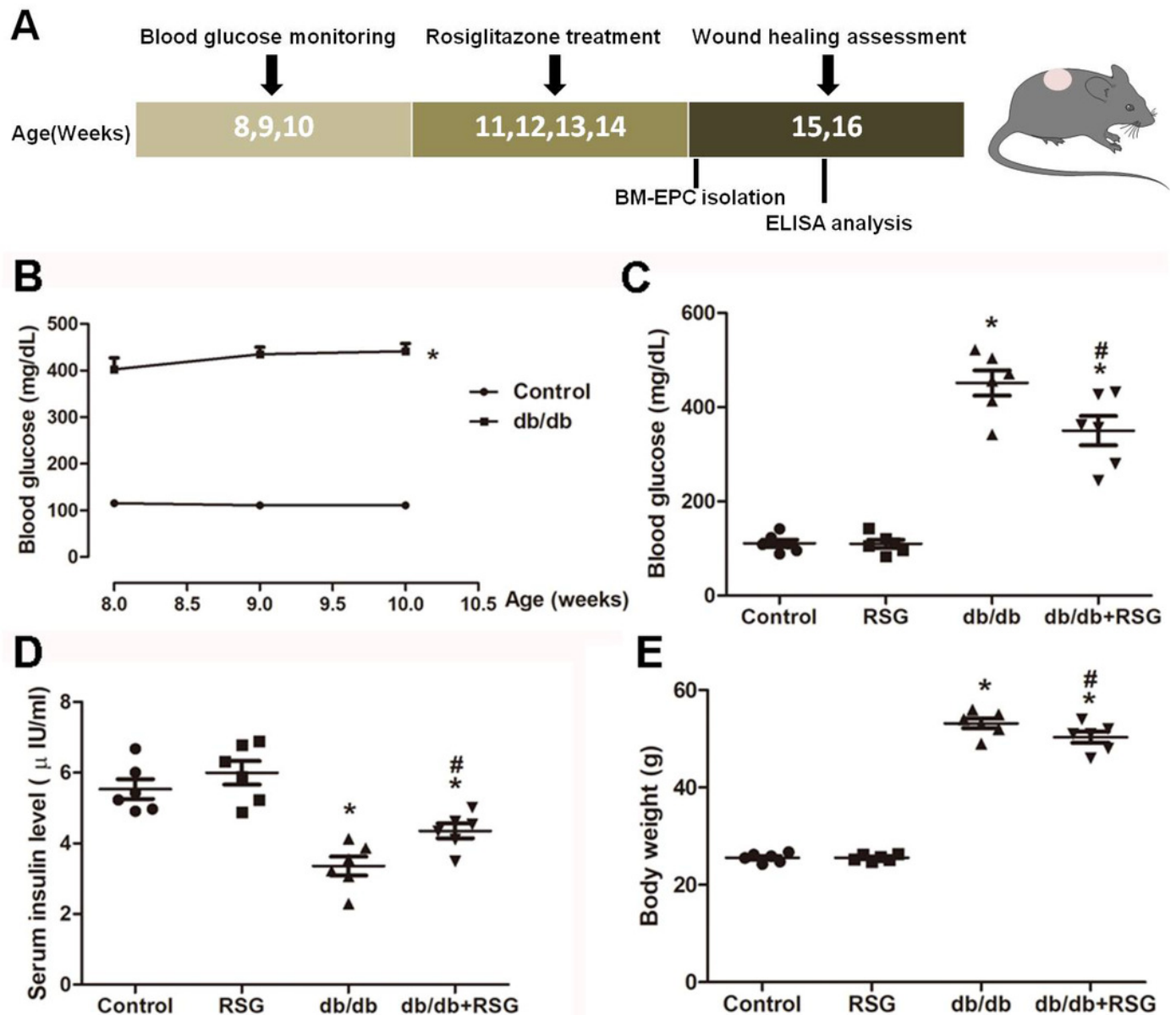
A

Blood glucose monitoring | Rosiglitazone treatment | Wound healing assessment

Age(Weeks) | 8,9,10 | 11,12,13,14 | 15,16

BM-EPC isolation

ELISA analysis

B

Blood glucose (mg/dL) vs Age (weeks)

- Control
- db/db

*

C

Blood glucose (mg/dL)

Control | RSG | db/db | db/db+RSG

*

#
*

D

Serum insulin level (μ IU/ml)

Control | RSG | db/db | db/db+RSG

*

#
*

E

Body weight (g)

Control | RSG | db/db | db/db+RSG

*

#
*

Figure 2

Rosiglitazone administration accelerated wound closure in *db/db* diabetic mice

After 4 weeks treated with RSG, *db/db* mice were produced a 6 mm circle wound on the dorsa by a punch biopsy and then pictures of the wound were taken every 2 days until day 14. RSG treatment accelerated wound closure in *db/db* mice. Representative pictures of wound closure on day 0, day 4, day8, day12 and day 14 (A-T) and quantitative analysis (U).

Values are mean ± SEM, (n=5 per group). $^{*}P$ <0.05 *vs.* Control; $^{#}P$ <0.05 *vs. db/db*. RSG, rosiglitazone.
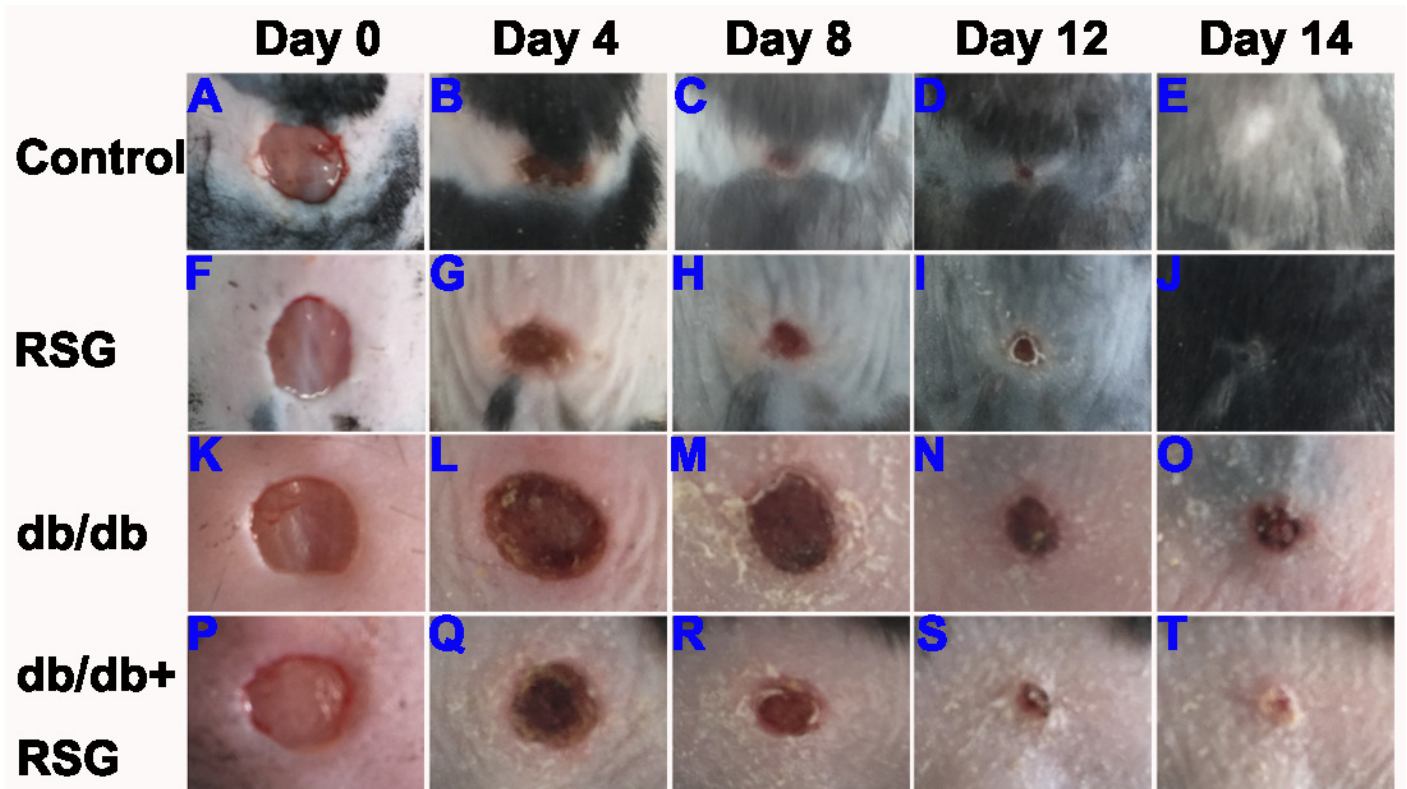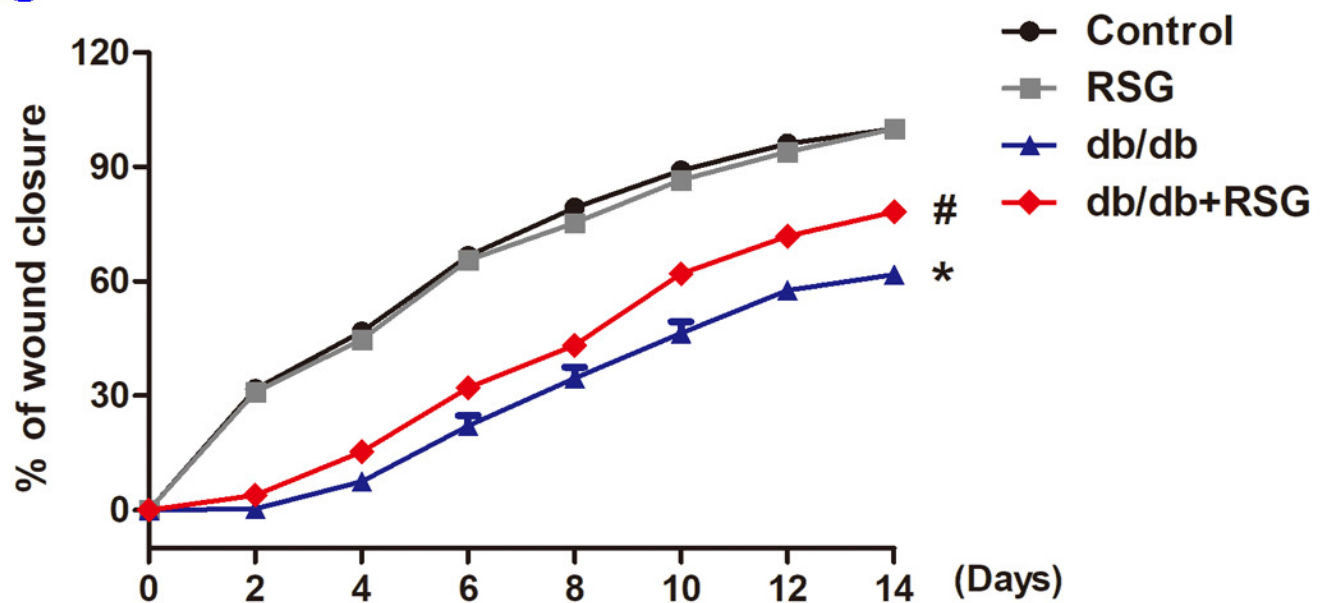
Figure 3

Rosiglitazone administration increased wound angiogenesis in *db/db* diabetic mice

In *db/db* mice, after wound closures were made, skins around the wound were collected and angiogenesis was evaluated on days 7 and 14. Representative pictures of tissue destruction of wounds (A, B) and CD31 staining (C-H). Quantitative study on day 7 (I) and day 14 (J). Red arrows point out CD31-positive capillaries (200×; scale bar, 50μm). Values are mean ± SEM, (n=5 per group). $^*P$ <0.05 *vs.* Control; $^\#P$ <0.05 *vs. db/db*. (&) Epidermis, (&&) dermis and (&&&) subcutis indicated. RSG, rosiglitazone. hpf, high power field.
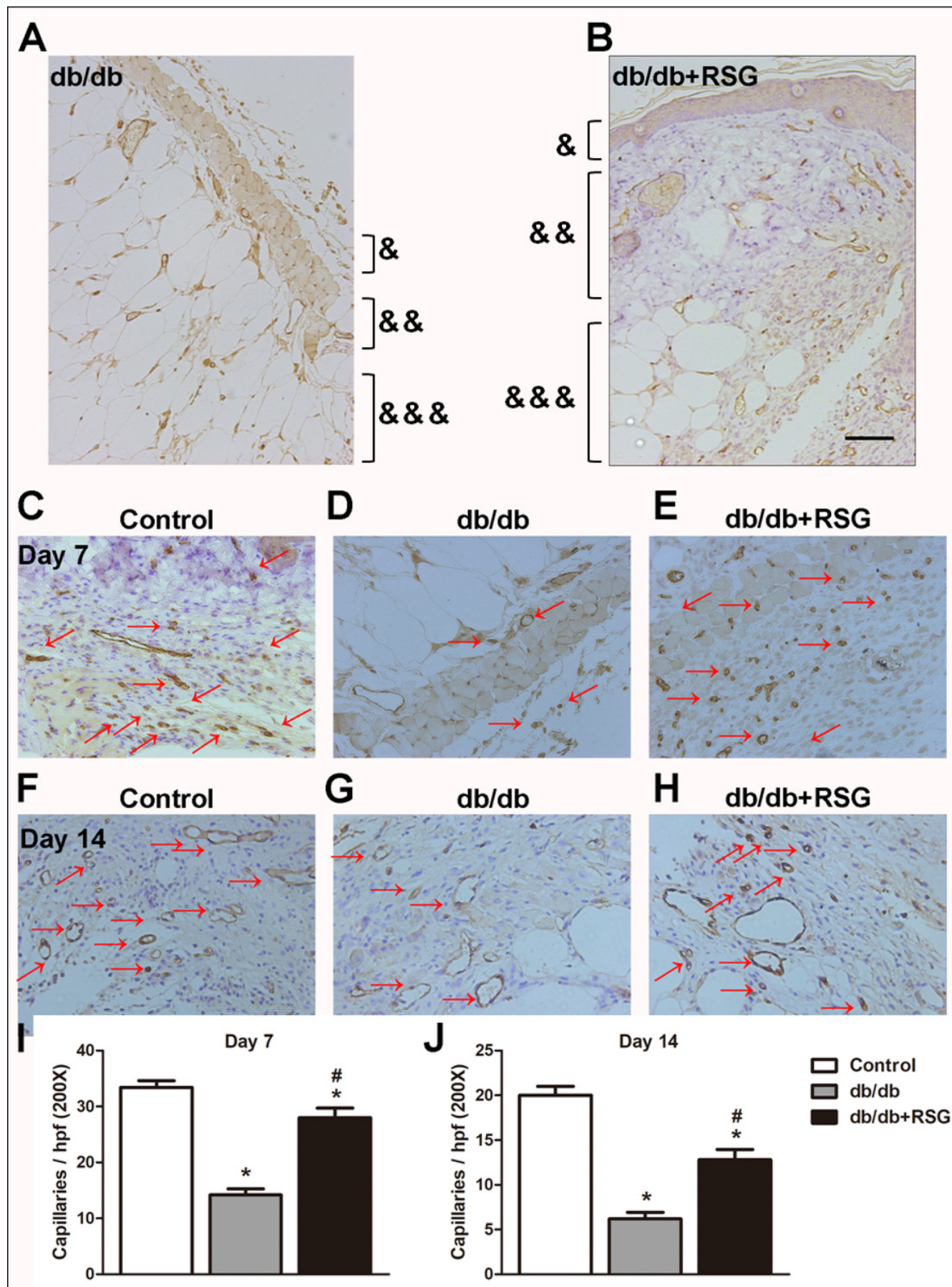
Figure 4

Rosiglitazone administration improved BM-EPC function in *db/db* diabetic mice

In *db/db* mice, BM-EPCs were isolated and cultured after 4 weeks RSG therapy. BM-EPC function was estimated by tube formation assay and migration assay. RSG treatment elevated tube formation ability (A-D, I) and migration ability (E-H, J) of BM-EPCs. A: 50×; scale bar, 100μm; B: 100×; scale bar, 100μm. Values are mean ± SEM, (n=6 per group). *P <0.05 *vs.* Control; #P <0.05 *vs. db/db*. RSG, rosiglitazone. lpf, low power field.
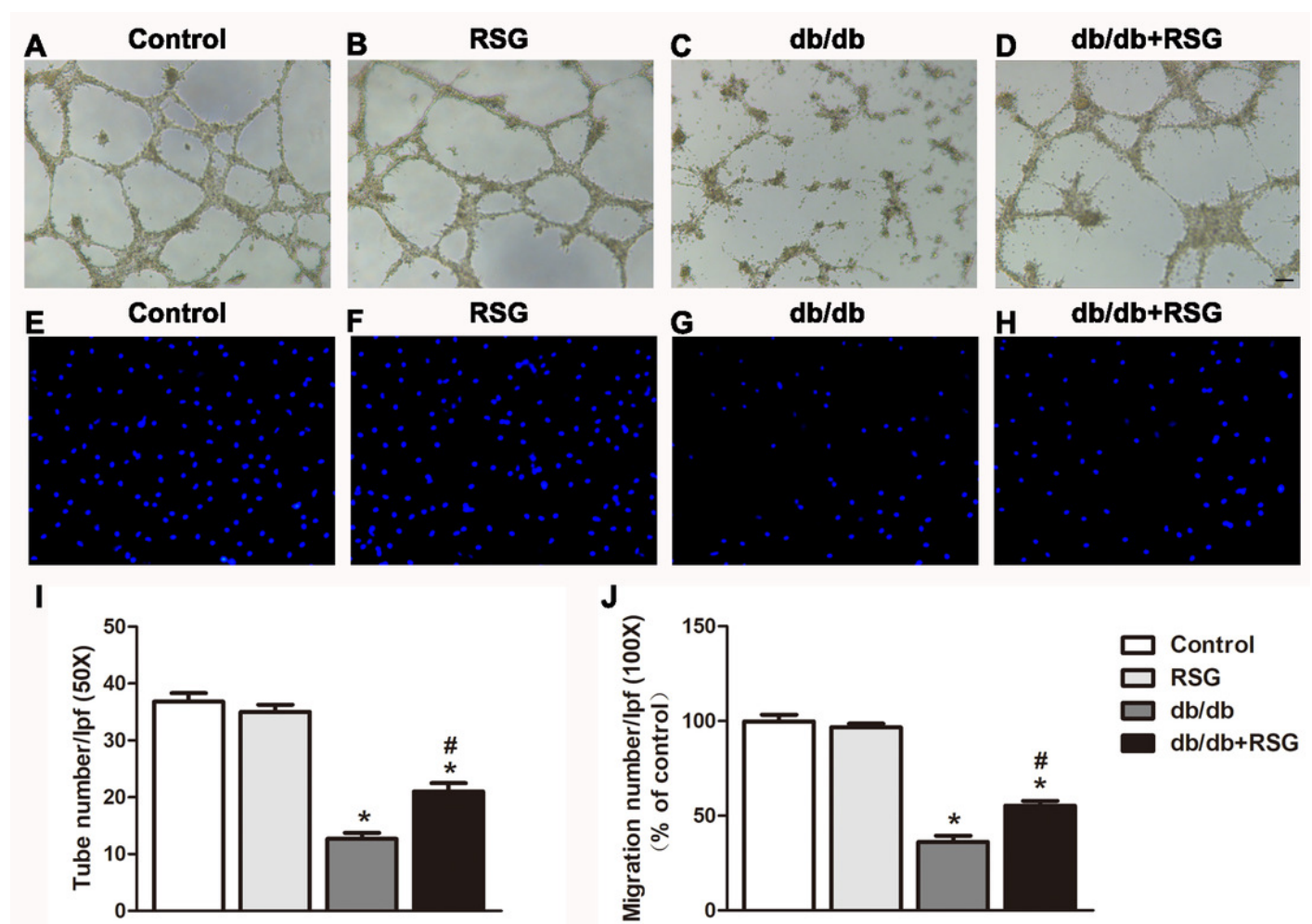
Figure 5

Rosiglitazone administration increases the levels of VEGF and SDF-1α protein and improved insulin resistant in *db/db* mice

(A) Effect of RSG treatment on SDF-1α protein levels in serum of the *db/db* mice. (B) ELISA analyses of VEGF levels in supernatant of BM-EPCs. (C) BM-EPCs treated with or without 1 μmol/L insulin for 1 h, and concentrations of phosphorylated AKT and total AKT were determined by the ELISA kit. Values are mean ± SEM, (A, B: n=6; C: n=5 per group). A, B: *P <0.05 *vs.* Control; A, B: #P <0.05 *vs. db/db*. RSG, rosiglitazone.
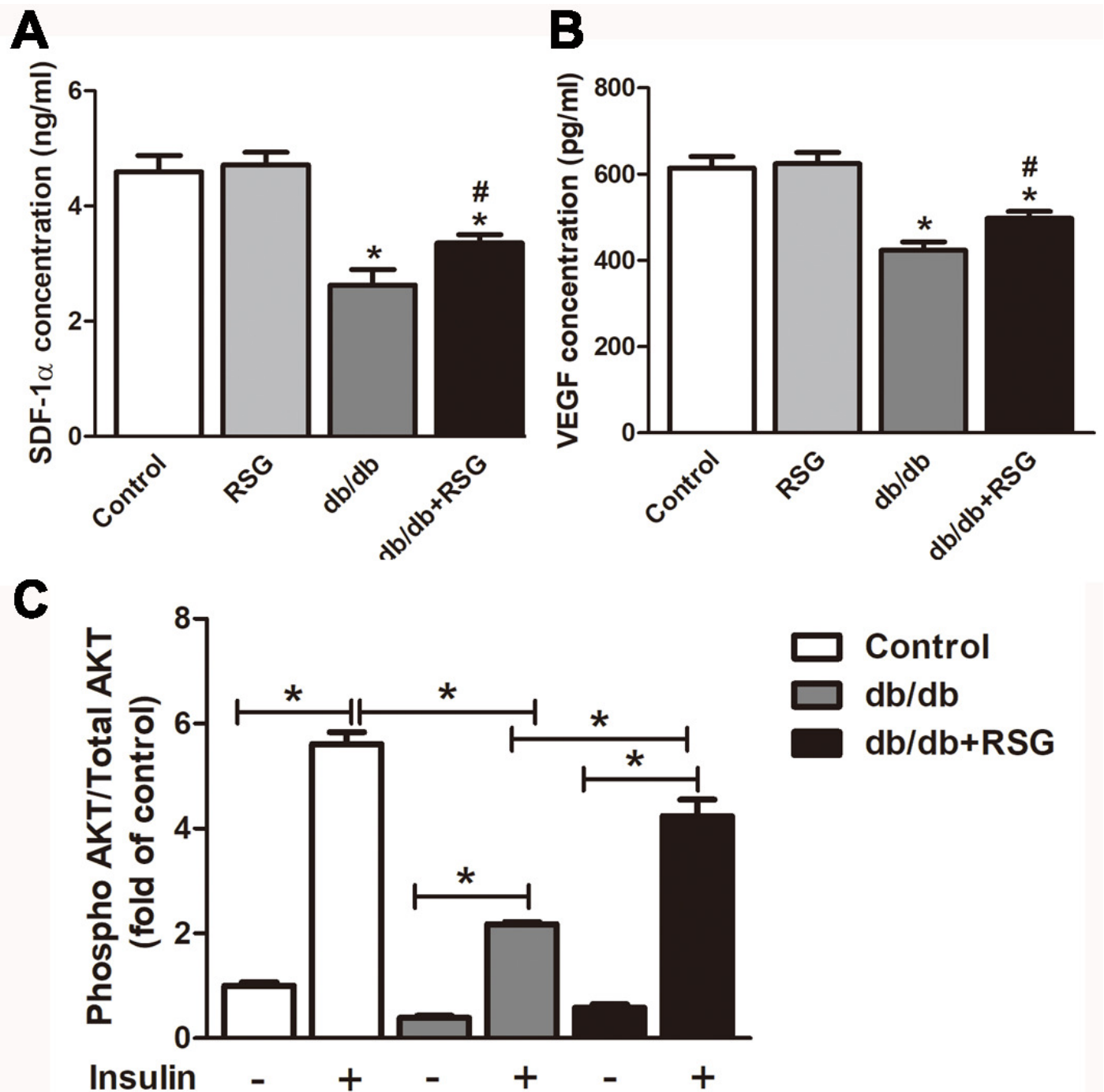
Figure 6

VEGF inhibitor avastin prevented the role of RSG in BM-EPCs induced by high glucose

(A) BM-EPCs exposed to 33 mmol/L glucose with or without RSG (10 nM) and VEGF inhibitor Avastin (25 µg/ml) for 24 h. CCK-8 detected EPC viability *in vitro*. (B-F) Avastin abolished the elevated tube formation ability by RSG (C-F: 50×; scale bar, 100µm). Values are mean ± SEM, (n=6 per group). RSG, rosiglitazone. HG, high glucose.